Calibration of capacitive humidity sensors for atmospheric sounding by remotely piloted vehicles

S. Mayer, J. Reuder and J. Schween
Meteorological Institute, Department of Physics, LMU Munich
September, 2005

Abstract

A miniaturized system for temperature and relative humidity measurements provided by remotely piloted vehicles has been tested under laboratory conditions by exposing it to different temperatures and humidities in a climatic exposure chamber using different saturated salt solutions. It is shown that the producer's conversion formular is not appropriate and therefore a calibration procedure is of great neccessity before the usage of the system.

1. Introduction

A measurement system on the basis of remotely piloted vehicles (RPVs) has been developed for sounding of the atmospheric boundary layer up to about 2 km above ground. The plane has a length of 1.29 m and a wing span of 2.10 m. The total mass is 3 kg. Flight velocities are in the range of 10-40 m s^{-1}. The optimum climb rate for highest altitude is 5 m s^{-1}. A sounding is normally completed within 15 min. The flight path during ascent is chosen to maximize the ascent height; that is, the pilots try to exploit slope winds and thermals. Descent is performed so as to equal time spans for ascent and descent. Egger et al. (2001). The RPVs are equipped with a sensor combination for measurement of temperature and relative humidity. Both sensors are mounted in a plastic tube of 23 mm length and 8 mm diameter, providing radiation protection and optimized approach flow to the sensors. The sensor combination has been purchased commercially from Ingenieurbüro D. Würtenberger, a manufacturer of miniature measurement instrumentation in the field of model aircraft. The underlying humidity sensor is the type HIH-3605-B produced by Honeywell Inc. For temperature measurements the type LM50 produced by National Semiconductor is used. Both sensors have the size of a pinhead, are extremely light and are outstanding for their little electricity consumption. Data acquisition and storage is done by a 8 channel 8-bit matchbox-sized data logger from Ingenieurbüro D. Würtenberger. This measuring system has already been used in in three field campaigns in Nepal 2001 (Egger et al. 2001), Bolivia 2003 (Egger et al. 2005) and Allgäu 2005 (Spengler et al. 2006). Before the field campaign was conducted in Bolivia 2003 the humidity sensors have been exposed to various temperature and humidity conditions to test the producer's specification.

2. Humidity Calibration

2a. *Method*

The humidity calibration method is based on the fact that a sealed off air volume in equilibrium with a supersaturated saline solution reaches a well-determined relative humidity (rh). Its value depends strongly on the selected salt and on the equilibrium temperature (T) of the system. The selection of the salts for our calibration procedure has been governed by two main aspects. First of all, a wide range of rh should be covered. Additionally, the salts should have a least as possible dependence on T, because there is a known, but in our opinion not accurately quantified, cross-sensitivity of the humidity sensor output to ambient temperature. A low temperature de-

pendence of the equilibrium humidity eases the determination of the temperature dependence of the sensor. Following these considerations we selected four salts with slight dependence on T, $LiCl$ (12.4 $\%$ @ 25 ^oC), $MgCl_2$ (33.2 $\%$ @ 25 ^oC), $NaCl$ (75.8 $\%$ @ 25 ^oC), and K_2SO_4 (96.9 $\%$ @ 25 ^oC) and one showing a distinct dependence on T, $Mg(NO_3)_2$ (53.4 $\%$ @ 25 ^oC). The corresponding rh given in percent are shown as a function of T in fig. 1.[1]

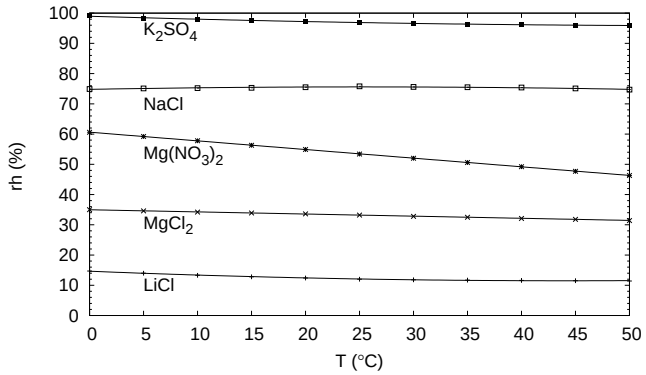

Figure 1: rh as a function of T over various supersaturated salt solutions. Lines represent derived polynomials of second order regression of the values given by Wexler and Hasegawa (1954).

2b. *Calibration system*

The main item of the calibration gadget is a stainless steel cylinder (Bender 1991) shown in fig. 2, 3 and 4. The removable lid is fixed by six screws, a O-ring seal provides hermetically enclosure of the inside air volume. The lead-through for the wires of the sensors is sealed with silicone. Mixing of the air inside the calibration chamber is enforced by a ventilator. The various supersaturated salt solutions are prepared in glass vessels, which can be easily inserted and replaced within the steel cylinder. During the calibration procedure the calibration gadget as a whole is mounted inside the climate exposure test cabinet of the Meteorological Institute in Munich.

Figure 2: Calibration gadget in the climatic exposure cabinet.

Figure 3: Sensors and propeller are fixed into the removable lid.

2c. *Measurements*

For each saline solution a calibration cycle covering T in the range between 0 ^oC, and 30 ^oC, is performed. The cycle starts at a temperature of 20 ^oC, which is held constant for 4 hours. During the following hour T of the

[1] Wexler and Hasegawa measured the humidity in the atmosphere above eight saturated salt solutions for ambient temperatures 0 to 50 ^oCusing a dewpoint hygrometer. Later, Greenspan compiled, from the literature, data on 28 saturated salt solutions to cover the entire range of relative humidity. Using a data base from 21 separate investigations comprising 1106 individual measurements, fits were made by the method of least squares to regular polynomial equations to obtain the "best" value of relative humidity in air as a function of temperature.

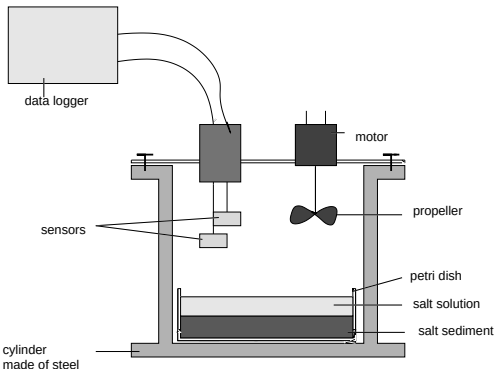

Figure 4: Closed calibration gadget is shown in a scematic cross section.

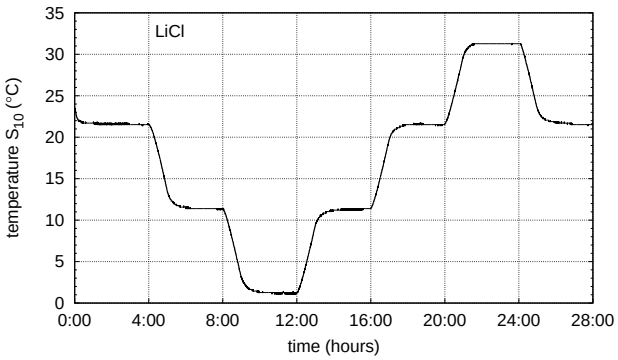

Figure 5: Example of a calibration cycle over LiCl showing T measured by the temperature sensor 10 (S_{10}) versus time.

climate chamber is gradually reduced to 10 ^oC, and held constant for another 3 hours. This procedure of a one hour temperature change and three hours of constant temperature is repeated for temperatures of 0 ^oC, 10 ^oC, 20 ^oC, 30 ^oC, and back to 20 ^oC, again (shown in fig. 5 for one sensor over LiCl). Thus, the overall cycle for each of the five saline solution takes a total of 28 hours. The length of the relaxation time intervals of three hours was chosen to ensure homogeneous T conditions for all components of the calibration chamber, especially the saline solution and the calibration air volume. Fig. 6 shows the development of the humidity sensor's voltage for a complete calibration cycle over LiCl. The voltage is increasing with decreasing T and vice versa before the equilibrium conditions are obtained. This can be explained by the fact that the air in the closed system warms or cools faster compared to the solution due to differences in their heat capacities. For the evaluation, the data set of the last 30 minutes for every temperature step was used by taking an arithmetical average of the sensors' voltage and the temperature $\bar{T}$, as well. $\bar{T}$ was used to calculate the necessary reference humidity after Wexler and Hasegawa rh_{ref} by using the polynomials which were obtained as shortly described before/forehand. To be able to calculate rh by the measured voltage of the capacitive humidity sensor the producer gives a linear function

$$rh = \frac{U_{out}}{U_{supply}} \cdot A + B \tag{1}$$

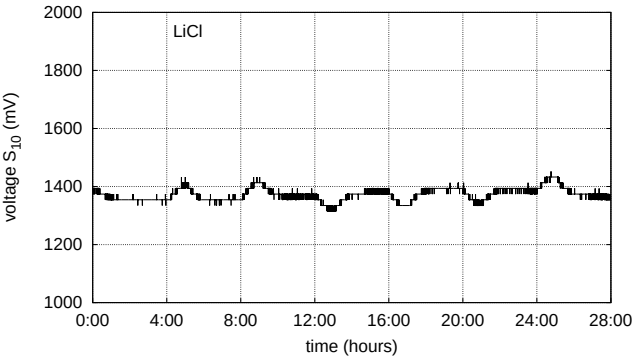

Figure 6: Voltage of humidity sensor S_{10} during a calibration cycle over LiCl.

with $A = 161.3$ and $B = -25.8$. U_{out} is the measured voltage of the sensor and U_{supply} is the voltage supply of the hereby/therefor used data minilogger. Honeywell provides for each sensor a function to correct the temperature dependence

$$f(T) = \frac{rh}{C + D \cdot T} \tag{2}$$

with $C = 1.0546$ and $D = -0.00216$. By using eq. (1) and eq. (2), the result is a distinct deviation Δ_{rh} from the reference humidity given by Wexler and Hasegawa (1954). All values are higher than the reference humidity. Es-

pecially for high voltage ranges between 4000 and 4500 mV (i.e. for high relative humidity) the deviation is high (between 7.5% and 18.5%) and depends on temperature (see fig. 7). Applying the temperature correction of Honeywell to the originally determined values of the humidity, the deviations decrease in average, but still they are with 1.5% upto 12% well above the demanded accuracy of $\pm 2\%$. This is not acceptable for RPV-based measurements of the relative humidity in the atmospheric boundary layer.

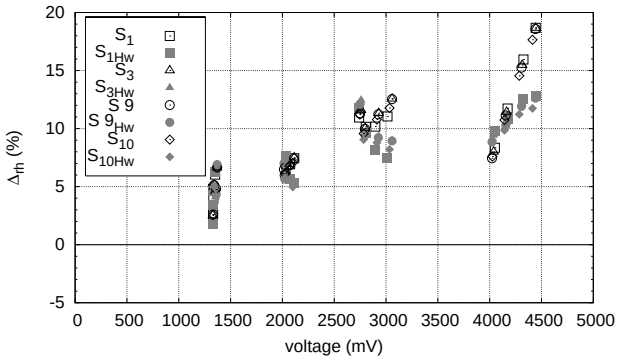

Figure 7: Comparison of measured relative humidities with and without temperature adjustment (indexed with Hw) referring to the theoretically correct humidity rh_{ref} given by Wexler and Hasegawa (1954) for four capacitive humidity sensors.

2d. *Determination of calibration constants*

The subsequent calibration calculations for the humidity sensors are based on the averaged sensor output values over the last 30 minutes of the corresponding constant temperature interval. First of all, the relative humidity given by Hasegawa versus the voltage of the capacitive humidity sensor is shown. For every temperature a linear regression was done. Fig. 8 shows this for S_{10}. The different slopes in the regression show the temperature dependence of the sensors. By executing a ploynamial regression of second order for the slopes $a(\bar{T})$ and offsets $b(\bar{T})$, for every sensor six new coefficients a_i and b_i ($i = 0, 1, 2$) can be determined. Thus, a new calibration function rh_c can be provided to calculate rh by voltage

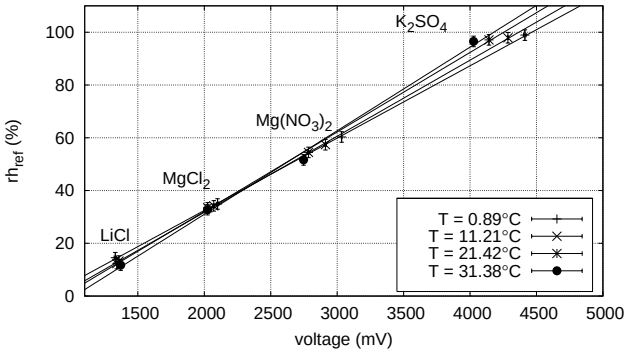

Figure 8: Signal voltage of the humidity sensor S_{10} versa the reference relative humidity over various salt solutions and for different temperatures.

and T.

$$rh_c = \underbrace{(a_2 \cdot T^2 + a_1 \cdot T + a_0)}_{=a(T)} \cdot U + \underbrace{b_2 \cdot T^2 + b_1 \cdot T + b_0}_{=b(T)} \quad (3)$$

Fig. 9 shows the distinct improvement in the humidity de-

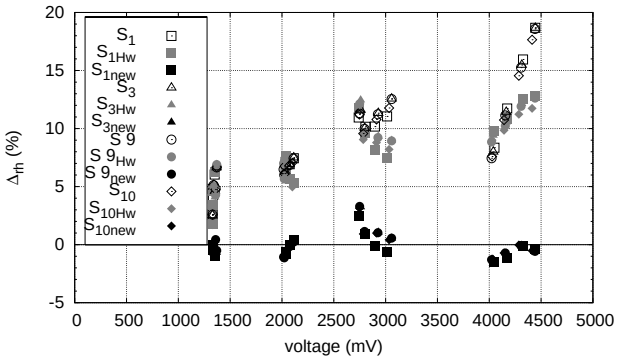

Figure 9: as in fig.7. In addition, deviations of the humidity determined with eq. (3) are shown with filled symbols.

termination with the described method. Unlike, the (old) values given by using the function of Honeywell (these values are indexed with Hw), now the deviation of almost all the values is between $\pm 2\%$.

3. Conclusions

Due to the fact, that the tested capacitive humidity sensors do not satisfy an accuracy of $\pm$ 2 % by applying the producer's formular (eq. 1) the shown calibration procedure is suggested to conduct before using the capacitive humidity sensors.

4. Acknowledgment

Special thanks to Anton Lex for his technical support in setting up the steel cylinder.

5. References

Bender S., 1991: Experimentelle Untersuchungen zur Feuchtemessung auf der Basis kapazitiver Messsonden mit polymerem Dielektrikum. Diplomarbeit für Meteorologie, LMU München.

Egger J., S. Bajrachaya, R. Heinrich, P. Kolb,S. Lämmlein, M.Mech, J.Reuder, W. Schäper, P. Shakya, J. Schween, H. Wendt, 2001: Diurnal Winds in the Hamalayan Kali Gandaki Valley. Part III: Remotely Piloted Aircraft Soundings. Mon. Wea. Rev., 130, 2042-2058.

Egger J., L. Blacutt, F. Ghezzi, R. Heinrich, P. Kolb, S. Lämmlein, M. Leeb, S. Mayer, E. Palenque, J. Reuder, W. Schäper, J. Schween, R. Torrez, F. Zaratti, 2005: Diurnal circulation of the South American Altiplano. Part I: Observations. Mon. Wea. Rev., 133, 911-924.

Spengler T., M. Ablinger, J. Egger, J. Schween, G. Zngl, 2006: Thermally driven winds in the exit region of the Lech Valley (Bavarian Alps) observed during the field experiment AllGEx 2005.

Wexler A. and S. Hasegawa, 1954: Relative Humidity-Temperature Relationships of Some Saturated Salt Solutions in the Temperature Range 0C to 50C. J. Res. Nat. Bur. Standards, Vol. 53, 19, RP 2512.